

Tomographic measurement of breakthrough in a packed bed adsorber

Karijm Salem^a, Evangelos Tsotsas^b, Dieter Mewes^{a,*}

^a*Institute of Process Engineering, University of Hannover, Callinstrasse 36, D-30167 Hannover, Germany*

^b*Thermal Process Engineering, University of Magdeburg, Universitätsplatz 2, D-39106 Magdeburg, Germany*

Received 10 September 2003; received in revised form 30 July 2004; accepted 4 August 2004

Available online 1 October 2004

Abstract

The tomographic measurement technique enables the measurement of local water vapour concentrations at the exit of a packed bed adsorber using near infra-red. This is realized by extending the adsorption column with a hollow glass cylinder that serves as the measurement cross-section. The glass is transilluminated from three directions with three light-sheets. The light absorption by water vapour is measured with three InGaAs photodiode arrays and these projections are used for the tomographic reconstruction of the concentration fields. For low water vapour concentrations ($c < 9E - 4$ mol/l) an error below 8% is reported. Concentration field measurements during adsorption show the early breakthrough near the column wall due to channeling effects at a low ratio between tube and particle diameter. © 2004 Elsevier Ltd. All rights reserved.

Keywords: Adsorption; Packed bed; Zeolites; Tomography; Near infra-red; Water vapour

1. Introduction

Adsorption is an important operation for purification and bulk separation of gas mixtures, usually conducted in packed beds. To effectively design the process, detailed analysis of the bed dynamics and kinetic data are required. With regard to the packed bed and especially in the case of high loads and a considerable heat release, the use of columns with a relatively low ratio between tube and particle diameter may be necessary. Then, channelling effects occur and the consideration of temperature and concentration profiles only with respect to the axial coordinate of the bed or to time is not sufficient; radial profiles across the tube must also be accounted for (Tsotsas and Schlünder, 1990; Winterberg and Tsotsas, 2000).

Local measurement techniques can only measure the concentration at certain locations, and often interference of the flow field by the measurement sensor cannot be avoided. To obtain information on a complete cross-section of an apparatus, numerous measurements must be taken by placing

the measurement probe at different locations. Therefore, only time-averaged information is available and can lead to misinterpretations, especially for the nonstationary flow in the adsorption column (Münstermann, 1984; Lingg, 1995).

To overcome this intrinsic measurement problem, an optical tomography technique is developed to provide noninvasive, high temporal and spatial resolution concentration measurements over a complete cross-section. However, because of the optical accessibility of the flow, the measurement cross-section is limited to the adsorber exit.

Gas concentration measurement techniques are well developed, based on quantitative spectroscopy (Talsky, 1994) and they are already applied for tomography measurements. The increased development of cheap laser diodes with spectra in the near infra-red allows to detect numerous gas species (Werle et al., 1998). Kauranen (1994) reported the measurement of a stationary gas flow with a low O₂-concentration. Using only one beam and the two-tone frequency modulation method the concentration field is measured by traversing and rotating the measurement cross-section. Hindle et al. (2001) presented a tomography technique with fibreoptics to investigate the hydrocarbon concentration in a combustion chamber. The light is fanned out in 32 fibres and launched across the measurement space from four directions.

* Corresponding author. Tel.: +49-511-762-3638; fax: +49-511-762-3031.

E-mail address: dms@ifv.uni-hannover.de (D. Mewes).

Therefore a temporal resolution of 3000 frames per second is achieved.

Fast photodiode arrays with high temporal and spatial resolution allow the measurement of complete light-sheets in less than 1 ms. Implementing these detectors enables concentration measurements with a high temporal and spatial resolution.

2. Experimental technique

2.1. Experimental set-up

The experimental set-up consists of an evaporator as feed supply and an adsorption column ($D = 50$ mm diameter) (Fig. 1). The column is divided into three segments, each 200 mm high, which allows to investigate different adsorber heights. To force channelling in the adsorption column, a small ratio of tube to particle diameter is realized ($D/d_p = 11.1$). The adsorption column is equipped with spherical adsorbent particles (type molecular sieve 4 \AA) with a diameter of $d_p = 4.5$ mm. To achieve high loads of the adsorbent, water vapour is chosen as feed. Due to these conditions an uneven water vapour distribution at the adsorber exit occurs. To measure these water vapour concentration fields the tomographic measurement device is attached to the column exit.

2.2. Near infrared (NIR) tomography

The developed tomography technique is based on the attenuation of light by water vapour. The transmission T of laser light is given by the Lambert Beer's law:

$$T = \frac{I_\lambda}{I_{\lambda,0}} = e^{-\varepsilon_\lambda c \Delta l}, \quad (1)$$

where I_λ is the monochromatic laser intensity at wavelength λ , measured after propagating a path length Δl through a medium with an absorbing species with concentration c and an extinction coefficient ε_λ . $I_{\lambda,0}$ represents the measured intensity at reference conditions with $c = 0$ mol/l.

A strong absorption line for water vapour has been computed by GENSPECT model (Quine and Drummond, 2002) and HITRAN database (Rothman et al., 1998) (Fig. 2). This is located in the near infrared region at 1396 nm. Other major constituents of the gas flow like nitrogen, oxygen, carbon dioxide and argon show no absorption at this wavelength. To adjust the absorption line exactly, a temperature-controlled distributed feedback laser diode (DFB) is used as a light source. The DFB laser provides a very narrow line width in the order of 10 MHz and the wavelength can be tuned over 3 to 5 nm about the nominal operating wavelength 1396 nm by temperature and current. Back-reflections into the laser diode result in wavelength instabilities and can destroy the diode. To prevent this, a faraday-isolator is installed directly

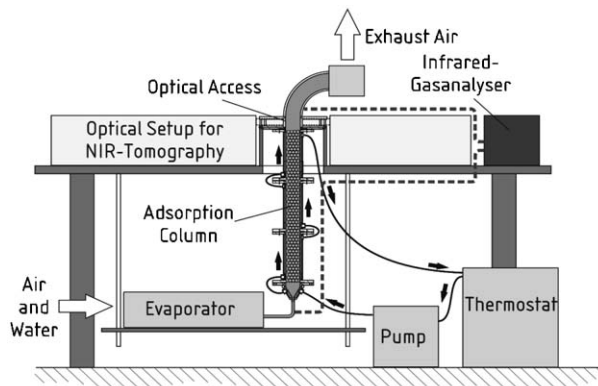


Fig. 1. Experimental set-up.

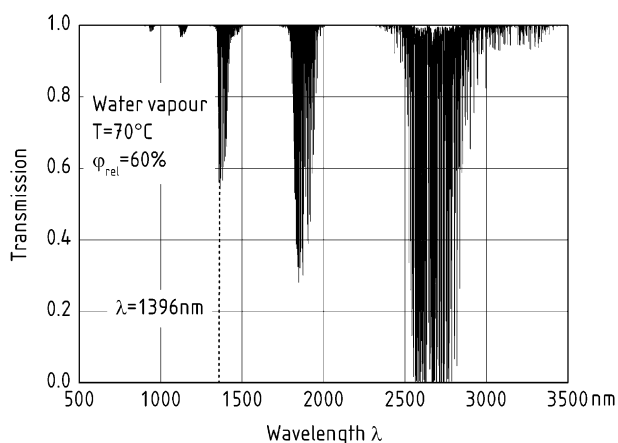


Fig. 2. Absorption spectrum of water vapour (HITRAN 1996).

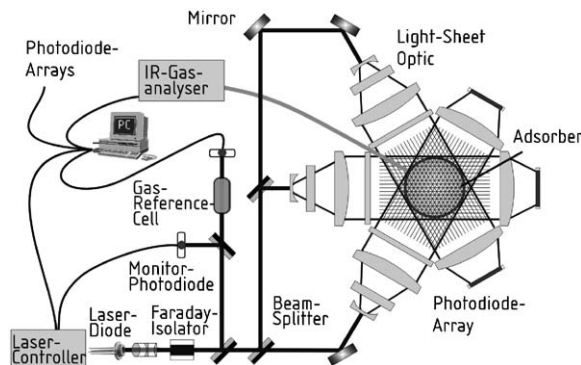


Fig. 3. Optical set-up for near infrared-tomography.

after the collimation optics and most lenses are coated with an anti-reflection layer.

The measurement cross-section is well-defined by a hollow glass cylinder (inner diameter 50 mm, thickness 1.8 mm), connected directly to the adsorption column (Fig. 3). The laser light is divided into three rays of equal intensity and the cross-section is transilluminated from three different directions using three light-sheets. The hollow

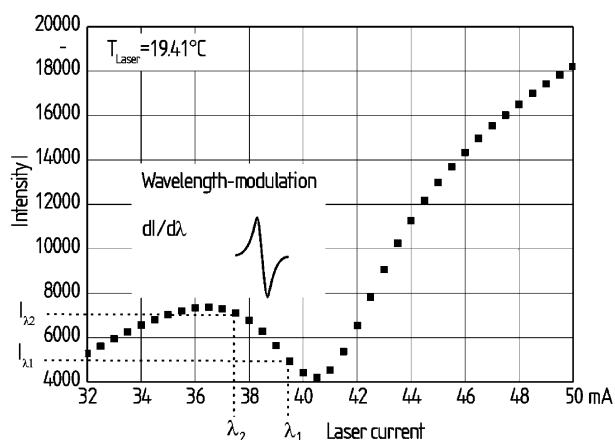


Fig. 4. Wavelength modulation for water vapour absorption line at 1396 nm.

glass cylinder itself operates as a lens and expands the light-sheets when entering and leaving. To achieve a parallel ray distribution in the hollow glass cylinder, the light-sheets are focused on the cylinder. Then, light is partially absorbed, depending on the water vapour concentration along the light paths. Behind the cylinder the light-sheets are focused on detector arrays with 6.4 mm width and 0.5 mm pixel height. Three 128 pixel InGaAs photodiode arrays measure the transmission along each light-sheet simultaneously. These three projections contain information about the concentration field in the measurement cross-section. To prevent the influence of surrounding water vapour in the air on the tomography device, the optics and laser are encased in a box which is purged with dry air.

During the measurements readjustment of the optics by vibrations and thermal effects can occur and decrease the signal quality significantly. To improve the signal quality the wavelength λ_1 is modulated by the laser current to a wavelength λ_2 with weaker absorption by water vapour (Fig. 4). Thus, the integrated concentration along a path length l can be expressed by

$$\int c dl = \frac{1}{(\epsilon_{\lambda_1} - \epsilon_{\lambda_2})} \ln \left[\frac{I_{\lambda_1,0} I_{\lambda_2}}{I_{\lambda_2,0} I_{\lambda_1}} \right], \quad (2)$$

where the intensities $I_{\lambda_1,0}$ and $I_{\lambda_2,0}$ are the measurement values at both wavelengths. The reference intensities I_{λ_1} and I_{λ_2} , the extinction coefficients ϵ_{λ_1} and ϵ_{λ_2} and the path length l are determined by calibration measurements.

2.3. Calibration method

To obtain as much information as possible from the measurement cross-section, the hollow glass cylinder is transilluminated up to 3 mm wall distance. This results in a disproportionate refraction for the fringe of the light-sheet. Therefore the measured ray distribution is no longer linearly related to the ray distribution in the measurement cross-section. The exact knowledge of the ray position is essential to conclude

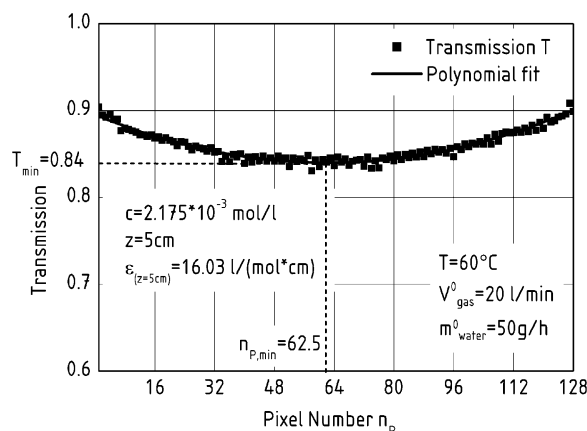


Fig. 5. Transmission profile for calibration.

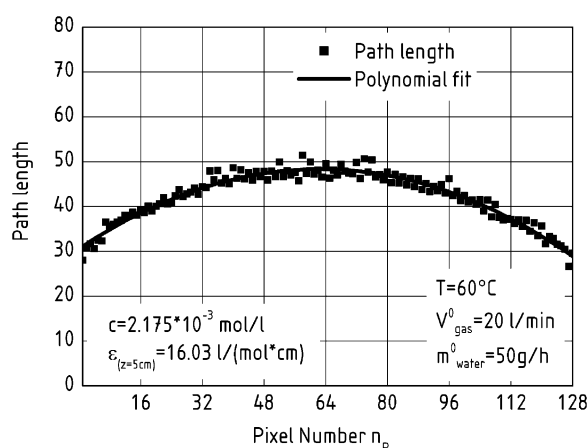


Fig. 6. Calculated path length profile.

on local concentrations of water vapour. To correct the distortion, a transmission measurement is recorded, while the cross-section is evacuated with a known water vapour concentration (Fig. 5).

The pixel at minimum transmission corresponds to the position of maximum path length in the measurement cross-section. The maximum path length in the measurement cross-section is 50 mm and given by the hollow glass cylinder geometry. This completes the necessary information to calculate the extinction coefficient by the Lambert Beer's law (Eq. (1)). The path length for each ray, represented by a detector pixel number is determined using the calculated extinction coefficient, the measured transmission data and the known water vapour concentration (Fig. 6).

2.4. Tomographic reconstruction

The tomography is used to reconstruct the two-dimensional concentration fields from the measured integral concentration along the ray paths. For the reconstruction the measurement cross-section is divided into triangular

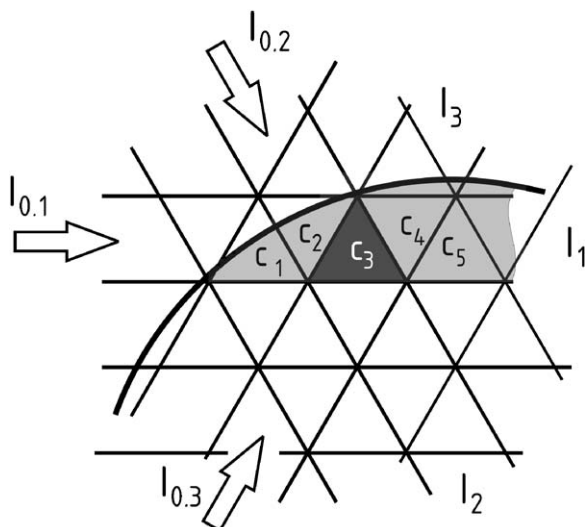


Fig. 7. Reconstruction grid with triangular elements.

elements. A good reconstruction quality and speed is achieved because each element belongs exactly to three rays and no weighting factors are needed. The arrangement of the elements is schematically depicted in Fig. 7.

The geometric partitioning into triangular elements requires equispaced rays in each light-sheet. Therefore, the distorted measurement data are equalized assigning the ray information to a theoretical triangular grid using the calculated path length. The reconstruction is done using the iterative algebraic reconstruction technique (ART), as shown by Buchmann and Mewes (1998, 2000). Starting from an assumed concentration distribution, the projections for this distribution are calculated. This theoretical set is then compared with the actually measured set. The difference between the two sets is fed into an optimizer where the assumed concentration distribution is corrected accordingly. This procedure is repeated until the standard deviation between the measured and the theoretical data set changes less than $10E-7$ mol/l. Hence, the deviation related to the measured concentration is always less than 1%. This error condition is usually met after 10 optimizations. Due to the small number of projection directions, the reconstruction is very sensitive to measurement errors. Especially, high concentration and temperature changes in the measurement cross-section during the experiment influence the refraction of rays in the light-sheet. These refraction changes as well as detector noise cause striations in the reconstructed image. While averaging of the measured data reduces the noise significantly, measurement errors by refraction changes can only be decreased by smoothing functions.

3. Results and discussion

To investigate the accuracy of the tomographic measurement results, constant water vapour concentrations in the

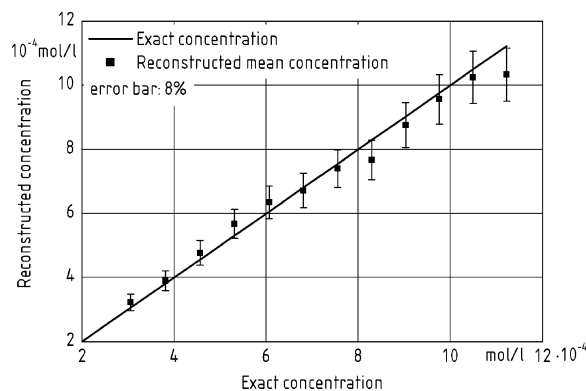


Fig. 8. Accuracy of the tomography results.

measurement cross-section are produced and measured. Low concentrations between $2E-4$ and $12E-4$ mol/l are realized. This corresponds to a relative humidity in the range between 16 and 84% at a temperature of 25°C . For these conditions absorption of laser light only up to 10% occurs at the maximum path length of 50 mm in the centre of the measurement cross-section. The measurement results for the different constant water vapour concentrations in the measurement cross-section in comparison with the exact concentration supplied by the evaporator are shown in Fig. 8. The error bars indicate a maximum error of 8% related to the exact concentration. The standard deviation of the concentration is $3.7E-5$ mol/l.

The results for an injected gas stream with a high water vapour concentration of $7.4E-4$ mol/l in a surrounding dry-gas stream are presented in Fig. 9. The dry-gas is flowing upwards through the measurement cross-section, while the injected stream flows in the opposite direction. The injection position is the centre of the measurement cross-section and the inner diameter of injection pipe amounts to 4 mm. Due to the opposite flow direction, the injected gas stream is mixed immediately with the surrounding dry gas and the maximum measured concentration is only $2E-4$ mol/l.

The concentration profiles and fields during adsorption are shown in Figs. 10a and b. One column segment with a height of 200 mm is used and filled with the spherical molecular sieve particles. Before the measurement the adsorbent particles are purged with a hot gas flow of 100°C for 3 h and then cooled to the measurement temperature of 60°C . All pipes and the column wall are temperature controlled to 60°C to avoid condensation of water vapour. Then the feed is adjusted to a constant relative humidity of 57% (at 60°C) and the adsorption column is charged. At the beginning of adsorption the column adsorbs the water vapour completely. After 79 s a concentration profile shows a strong increase of concentration at the column wall while the concentration in the centre of the column remains constant. This behaviour is the result of high velocities near the column wall due to channelling (Münstermann, 1984; Lingg, 1995). The mass and heat transfer between feed and adsorbent is increased, the adsorbent saturates and the feed breaks through. Five

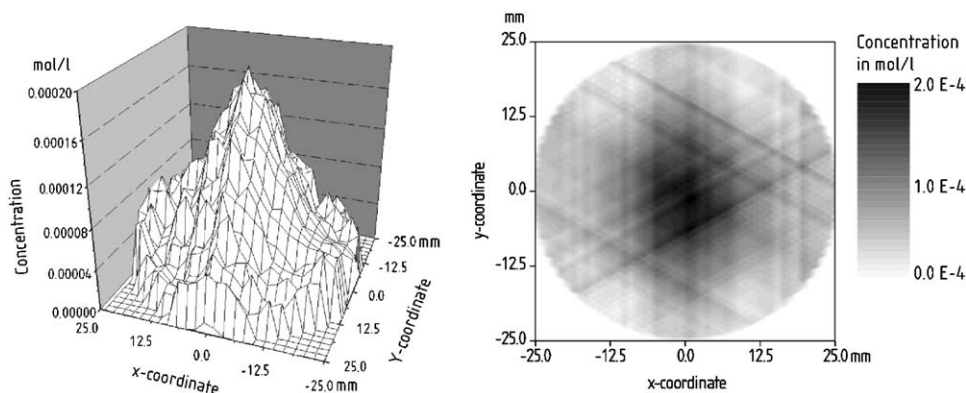


Fig. 9. Reconstructed concentration field for injected water vapour stream.

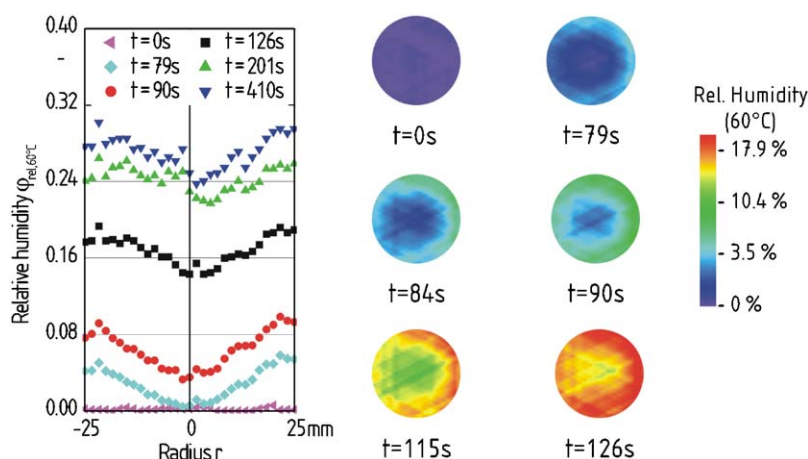


Fig. 10. Reconstructed concentration fields during adsorption process.

seconds later the adsorbent in the column centre saturates and the water vapour concentration in this region increases. With proceeding adsorption the concentration increases over the complete measurement cross-section. The adsorbent approaches the equilibrium and the concentration profiles flatten. The corresponding concentration fields show a symmetrical concentration distribution.

4. Conclusions

The developed tomographic measurement device in the near infrared enables water vapour concentration measurements in a circular measurement cross-section of only 50 mm. With this technique it is possible to investigate the breakthrough of a packed bed adsorber two-dimensionally. The tomography device is capable to measure low water vapour concentrations with an error of less than 8%. Concentration field measurements during adsorption show the early breakthrough near the column wall due to channelling effects at a low ratio between tube and particle diameter.

Acknowledgements

The financial support of the Deutsche Forschungsgemeinschaft (DFG) is acknowledged. The authors would also like to thank Zeochem AG, CH, for the supply of molecular sieve 4 Å.

References

- Buchmann, M., Mewes, D., 1998. Measurement of the local intensities of segregation with the tomographical dual wavelength photometry. *Canadian Journal of Chemical Engineering* 76 (3), 626–630.
- Buchmann, M., Mewes, D., 2000. Tomographic measurements of micro- and macromixing using the dual wavelength photometry. *Chemical Engineering Journal* 77 (4), 3–9.
- Hindle, F., Carey, S., Ozanyan, K., Winterbone, D., Clough, E., McCann, H., 2001. Measurement of gaseous hydrocarbon distribution by a near infra-red absorption tomography system. *Journal of Electronic Imaging* 10, 593–600.
- Kauranen, P., 1994. Tomographic imaging of fluid flows by the use of two-tone frequency-modulation spectroscopy. *Optics Letters* 19 (18), 1489–1491.
- Lingg, G., 1995. Die Modellierung gasdurchströmter Festbettadsorber unter Beachtung der ungleichmäßigen Strömungsverteilung und

- äquivalenter Einphasenmodelle. Dissertation, Technische Universität München.
- Münstermann, U., 1984. Adsorption von CO₂ aus Reingas und aus Luft am Molekularsieb-Einzelkorn und im Festbett. Dissertation, Technische Universität München, Germany.
- Quine, B.M., Drummond, J.R., 2002. GENSPECT: A line-by-line code with selectable interpolation error tolerance. *Journal of Quantitative Spectroscopy and Radiative Transfer* 74 (2), 147–165.
- Rothman, L.S., Rinsland, C.P., Goldman, A., Massie, S.T., Edwards, D.P., Flaud, J.-M., Perrin, A., Cammy-Peyret, C., Dana, V., Madin, J.Y., Schroeder, J., Mccann, A., Gamache, R.R., Wattson, R.B., Yoshino, K., Chance, K.V., Jucks, K.W., Brown, L.R., Nemtchinov, V., Varanasi, P., 1998. The HITRAN molecular stratospheric database and Hawks (HITRAN atmospheric workstation): 1996 edition. *Journal of Quantitative Spectroscopy and Radiative Transfer* 60 (5), 665–710.
- Talsky, G., 1994. *Derivative Spectrophotometry: Low and Higher Order*, VCH, Weinheim.
- Tsotsas, E., Schlünder, E.-U., 1990. Measurement of mass transfer between particles and gas in packed tubes at very low tube to particle diameter ratios. *Wärme-und Stoffübertragung* 25, 245–256.
- Werle, P., Mücke, R., Amato, F.D., Lancia, T., 1998. Near-infrared trace-gas sensors based on room-temperature diode lasers. *Applied Physics* 67, 307–315.
- Winterberg, M., Tsotsas, E., 2000. Modelling of heat transport in beds packed with spherical particles for various bed geometries and/or thermal boundary conditions. *Journal of Thermal Science* 39, 556–570.